The x-ray $K\beta_{2,5}$-emission band and the electronic structure of Zn, ZnS and ZnSe crystals

1996 J. Phys.: Condens. Matter 8 6791

(http://iopscience.iop.org/0953-8984/8/36/029)

J. Phys.: Condens. Matter **8** (1996) 6791–6801. Printed in the UK

The x-ray K$\beta_{2,5}$-emission band and the electronic structure of Zn, ZnS and ZnSe crystals

R Laihia†, J A Leiro‡, K Kokko† and K Mansikka†

† Department of Physics, University of Turku, FIN-20014 Turku, Finland
‡ Department of Applied Physics, University of Turku, FIN-20014 Turku, Finland

Received 27 March 1996, in final form 23 May 1996

Abstract. The present work deals with the x-ray K$\beta_{2,5}$-emission bands and the electronic structures of Zn metal as well as ZnS and ZnSe compounds. The measurements of the Zn K-emission bands were made with a two-crystal x-ray spectrometer and the electronic structures were calculated by using the linear muffin-tin orbital (LMTO) method. The above-mentioned compounds were chosen as the subject of the investigation because they are ideal materials for studying the 3d–4p hybridization since the Zn d band is about 10 eV below the Fermi level and therefore Kβ_2 and Kβ_5 are quite well separated from each other. We also suggest that the peak which is less than 9 eV below the same level in the experimental spectrum of the ZnS (ZnSe) compound is largely caused by the quadrupole radiation.

1. Introduction

Zn compounds (ZnS, ZnSe) are well-known materials in science and technology. ZnS is an important raw material in the mining industry for the production of Zn metal. ZnSe turns out to be a useful compound in semiconductor technology. Due to its wide band gap it is a promising material for the development of blue-light lasers [1–3]. X-ray emission spectra (XES) offer an ideal tool for the investigation of semiconductors and insulators because of the absence of charging effects. On the other hand these experiments give information on the electronic structure of the valence electrons. Furthermore, the measurements are site dependent as far as the different atomic types of the compounds are concerned. This site dependence is caused by the creation of the localized core hole of the specific atom by an x-ray photon.

In order to interpret the experimental x-ray emission bands, theoretical investigations are most important. The local partial density of states (DOS) gives information about the site-dependent electronic states. In the LMTO [4] band-structure calculation method the local partial DOS are obtained in a natural way. One of the first x-ray investigations of the K-emission bands of ZnSe is due to Drahokoupil and Šimůnek [5]. For recent investigations which deal with ZnS and ZnSe compounds we pay attention to references [6–11].

2. Experimental arrangements

The Zn K-emission band (K$\beta_{2,5}$) measurements were made with a two-crystal x-ray spectrometer. Two highly perfect Si(111) crystals in the first-order reflection were used as monochromators [12]. A sealed-off commercial x-ray fluorescence tube (Mo anode)

0953-8984/96/366791+11$19.50

was used for excitation. The applied voltage was 40 kV and the current 40 mA. The radiation was detected by means of a scintillation detector. The spectrometer chamber was continuously pumped to a pressure of about 10^{-3} Torr. The smallest possible rotation of the microprocessor-controlled spectrometer axes was $2''$. The final spectrum was the result of a summation of the pulses accumulated during about 400 sweeps. For one sweep 150 steps were needed (4 s per channel). Commercial Zn, ZnS and ZnSe polycrystalline samples with high purity were used for the measurements. The full width at half-maximum (FWHM) of the instrument function was estimated to be about 1 eV.

3. Methods of calculations

The calculations were performed by using the scalar-relativistic LMTO method including the combined correction terms and the atomic-sphere approximation (ASA). The basis function set for the valence electrons consisted of s, p and d functions. The core states were held fixed throughout the self-consistent cycles of the calculation. The exchange–correlation effects were introduced within the local density approximation using the von Barth–Hedin potential [13]. Since the zinc-blende structure is an open crystal structure we introduced empty spheres in the unit cell to decrease the overlapping volume of the atomic Wigner–Seitz (WS) spheres in the ASA approximation. Equal atomic WS radii were used for all atoms and empty spheres in ZnS and ZnSe compounds. The lattice parameters used in the calculations were $a = b = 2.66$ Å, $c = 4.95$ Å for pure Zn and $a = 5.41$ Å and $a = 5.67$ Å for ZnS and ZnSe compounds, respectively.

We made also a test calculation for the ZnSe compound including the f states in the basis set. However, the results below the Fermi level were practically the same as without the f states. The effect of the number of k-points and lattice vectors in the real- and reciprocal-space summations was tested as well. The self-consistent potentials were calculated by using 20 k-points in the irreducible wedge of the Brillouin zone and the final results were obtained by using 240 k-points. In the lattice sums we used about 3000 vectors.

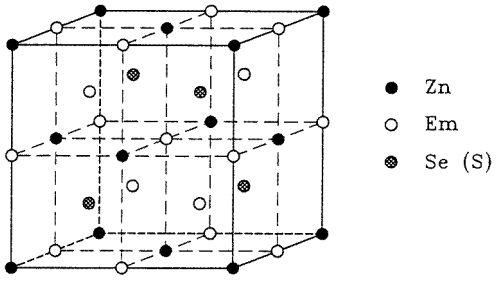

Figure 1. The unit cell of ZnS and ZnSe compounds. 'Em' means empty sphere.

In this paper the x-ray emission spectra and the electronic structures of pure Zn metal as well as ZnS and ZnSe compounds are studied. The crystal structures of pure Zn and both compounds are hexagonal (HCP) and cubic zinc-blende (ZnS), respectively. However, since the ZnS structure is a relatively open structure we have to introduce empty spheres in the unit cell to perform the calculations properly. By using these empty spheres it is possible to treat the ZnS structure as a BCC-type structure with a high packing density (figure 1).

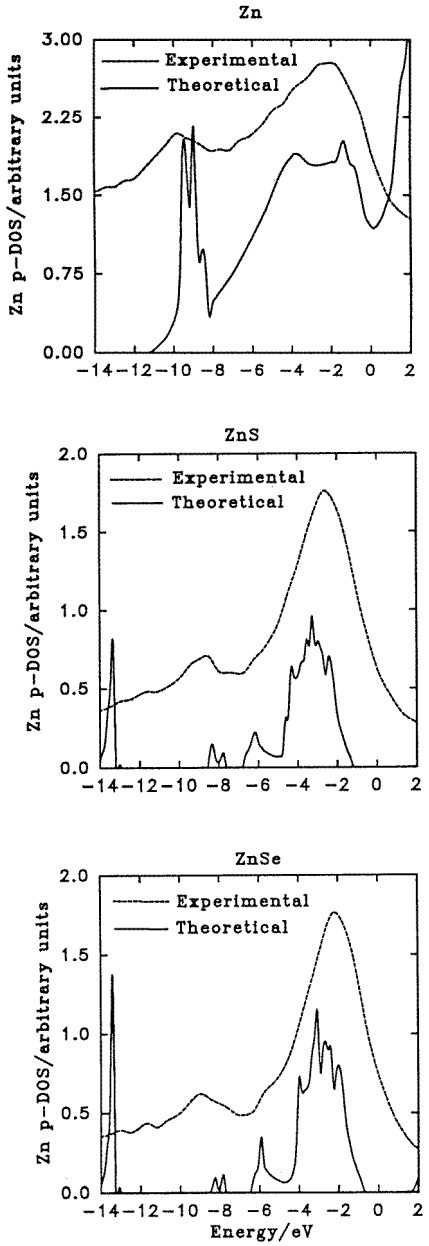

Figure 2. X-ray K-emission bands and the theoretical Zn p density of states (p-DOS) in Zn, ZnS and ZnSe as functions of energy. The Fermi level is at 0 eV.

4. Results

4.1. Experimental results

In x-ray emission the intensity of the radiation is modified by the matrix element $\langle \mathrm{f}|\exp(-\mathrm{i}\boldsymbol{k}\cdot\boldsymbol{r}_i)\boldsymbol{\epsilon}^{(\alpha)}\cdot\boldsymbol{p}_i|\mathrm{i}\rangle$ [14], where $\langle \mathrm{f}|$ and $|\mathrm{i}\rangle$ refer to the final and initial states of

the electronic system, $\boldsymbol{k}$ and $\boldsymbol{r}_i$ are the wave vector of the emitted x-radiation and the position of the ith electron, respectively, $\boldsymbol{\epsilon}^{(\alpha)}$ is the linear polarization vector and $\boldsymbol{p}_i$ is the momentum operator. Expanding the exponential function in terms of a power series $\exp(-\mathrm{i}\boldsymbol{k}\cdot\boldsymbol{r}_i) = 1 - \mathrm{i}\boldsymbol{k}\cdot\boldsymbol{r}_i - (\boldsymbol{k}\cdot\boldsymbol{r}_i)^2/2 + \cdots$ leads to a series representation of the matrix element. In this series the first term is the dipole term. The electric part of the second term containing $\mathrm{i}\boldsymbol{k}\cdot\boldsymbol{r}_i$ is called the quadrupole term. The dipole term gives a nonzero contribution if the l quantum numbers of the $\langle\mathrm{f}|$ and $|\mathrm{i}\rangle$ states differ by one ($\Delta l = \pm 1$, dipole selection rule). The quadrupole term leads to nonzero contribution if $\Delta l = \pm 2$. For soft x-rays (small $\boldsymbol{k}$) the quadrupole and higher terms are small compared to the dipole term which gives the leading contribution to the observed spectrum.

Let us first consider the K$\beta_{2,5}$ spectrum of pure Zn metal. The dipole selection rule is assumed to be approximately valid in x-ray emission spectroscopy. This makes it possible to investigate the electronic structure in the framework of the partial DOS and transition matrix elements. In high-energy x-ray spectroscopic studies some quadrupole lines may be found since the dipole selection rule may be only approximately valid. The intensity of the quadrupole line ($1\mathrm{s}^{-1} \rightarrow 3\mathrm{d}^{-1}$, a hole moves from the 1s to the 3d states) should be lower than that of the corresponding dipole line ($1\mathrm{s}^{-1} \rightarrow 4\mathrm{p}^{-1}$). Usually, the K$\beta_5$ spectrum is associated with the quadrupole selection rule and the Kβ_2 spectrum with the dipole selection rule.

The experimental K-emission band possesses the lifetime broadening of the 1s level, which has been calculated to be about 1.67 eV [15]. In addition, the effect of the instrument function is of the same order of magnitude. Therefore, the experimental spectra are smoother than the theoretical ones. Let us consider the Zn K$\beta_{2,5}$ spectrum shown in figure 2. Two features, which we call as Kβ_2 and Kβ_5 according to their energy region, can be clearly separated from the experimental spectrum. The latter one has the binding energy 9.8 ± 0.3 eV as measured from the Fermi level discontinuity point. In the present work we mean by binding energy the energy relative to the Fermi energy. The intensity ratio between the Kβ_5 and Kβ_2 contributions can be estimated to be only $10 \pm 1\%$. This shows the dominance of the dipole selection rule for the experimental Zn K-emission band.

The corresponding K$\beta_{2,5}$ spectrum for ZnSe at the sites of Zn atoms is shown in figure 2 as well. The Kβ_5 part of the spectrum is now at 8.9 ± 0.3 eV below the Fermi level of pure Zn. Moreover, the intensity of the Kβ_5 spectrum relative to that of the Kβ_2 one is $(8 \pm 1)\%$, which is just slightly smaller than that for pure Zn. Furthermore, the overall K$\beta_{2,5}$ spectrum is narrower than that of Zn as well. This means that the valence electrons are more localized at the site of Zn atoms in the case of the semiconductor ZnSe.

Let us now turn to the Zn K$\beta_{2,5}$ spectrum of the insulator ZnS, which is quite similar to that of ZnSe. As can be seen from figure 2 the binding energy of Kβ_5 is (8.5 ± 0.3) eV and the Kβ_5/Kβ_2 ratio can be estimated to be $7\pm1\%$. This intensity ratio is not so much smaller than that of pure Zn although the theoretical results show a rather small hybridization effect between the Zn 4p and 3d bands of ZnS as compared with the pure Zn case. One can also note a small hybridization feature at about 6 eV below the Fermi level in between the Kβ_5 and Kβ_2 spectra which is in good overall agreement with the calculated p partial density of states. The possible transition matrix element effects can be assumed to be quite small in this energy region of the spectrum as well [16].

4.2. Theoretical results

The calculated partial DOS of Zn, ZnS and ZnSe are shown in figures 3–5. Zn is a typical semi-metal with a narrow, deep-lying d valence band. S is a nonmetal and Se is

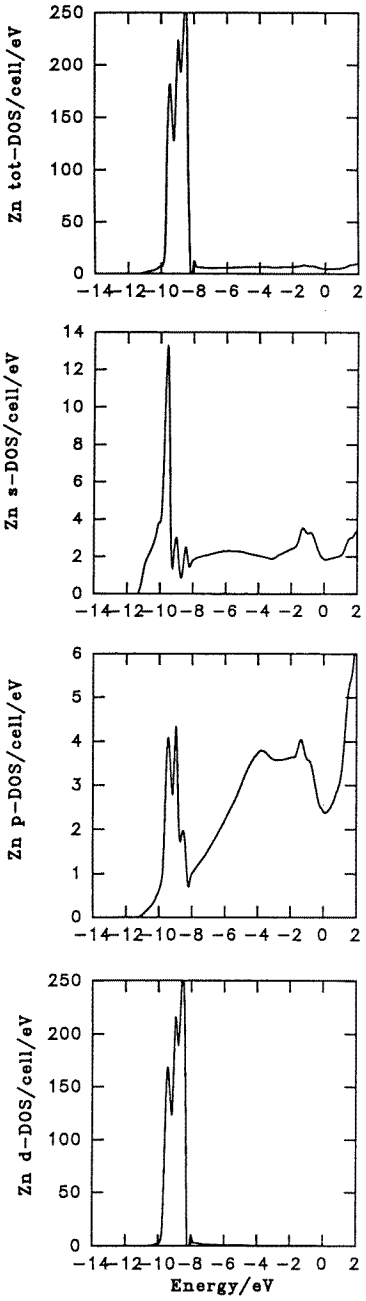

Figure 3. The total DOS (tot-DOS) and the partial s-, p- and d-DOS of Zn.

a semiconductor and they both have a narrow s band which lies even deeper than the Zn d band. Since Zn is one of the group IIB metals and both S and Se belong to the group VIB they are good candidates for making II–VI compound semiconductors. The present calculations give 2.0 eV and 1.3 eV for the ZnS and ZnSe band gaps between the valence

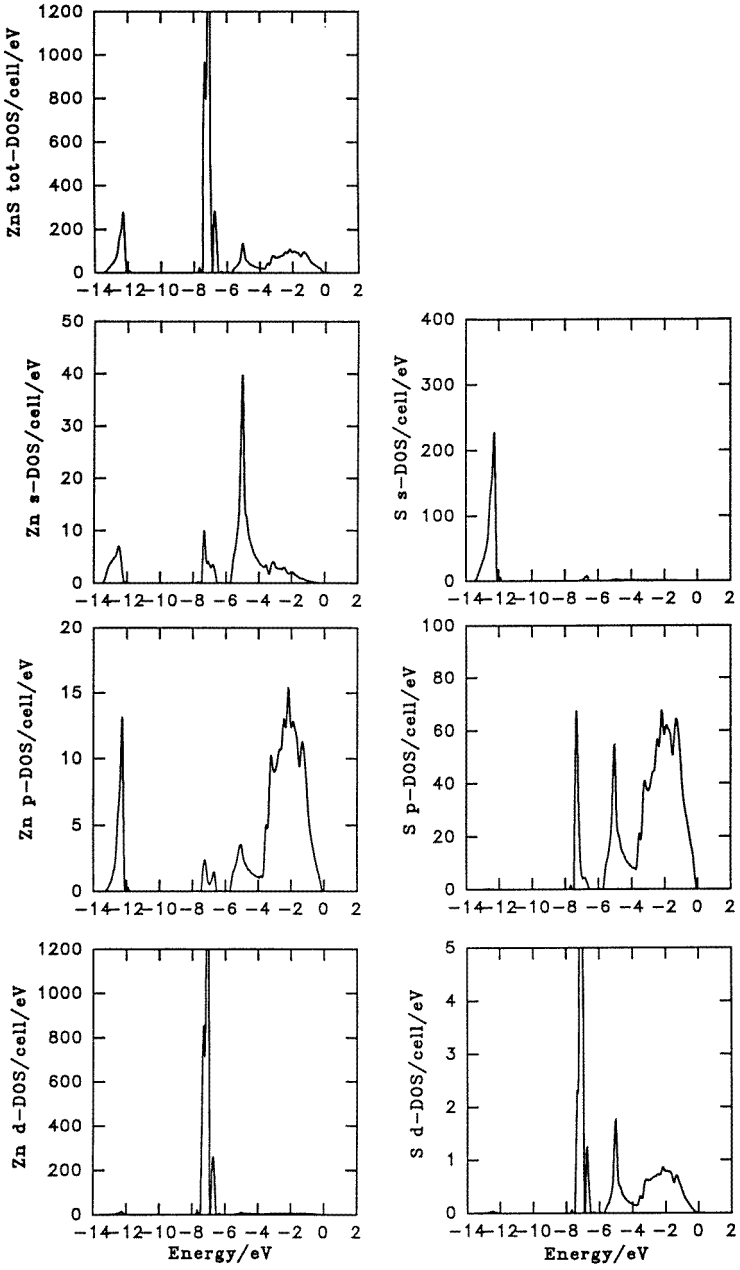

Figure 4. The tot-DOS of ZnS and the partial s-, p- and d-DOS of Zn and S in ZnS.

and conduction bands, respectively.

In the following we consider only the occupied part of the calculated band structure since the x-ray emission experiments, discussed earlier, provide information only on the occupied states. We start by considering the total DOS (figures 3–5). In pure Zn the occupied part of the valence band forms a continuous band structure with the 3d states lying at the bottom of

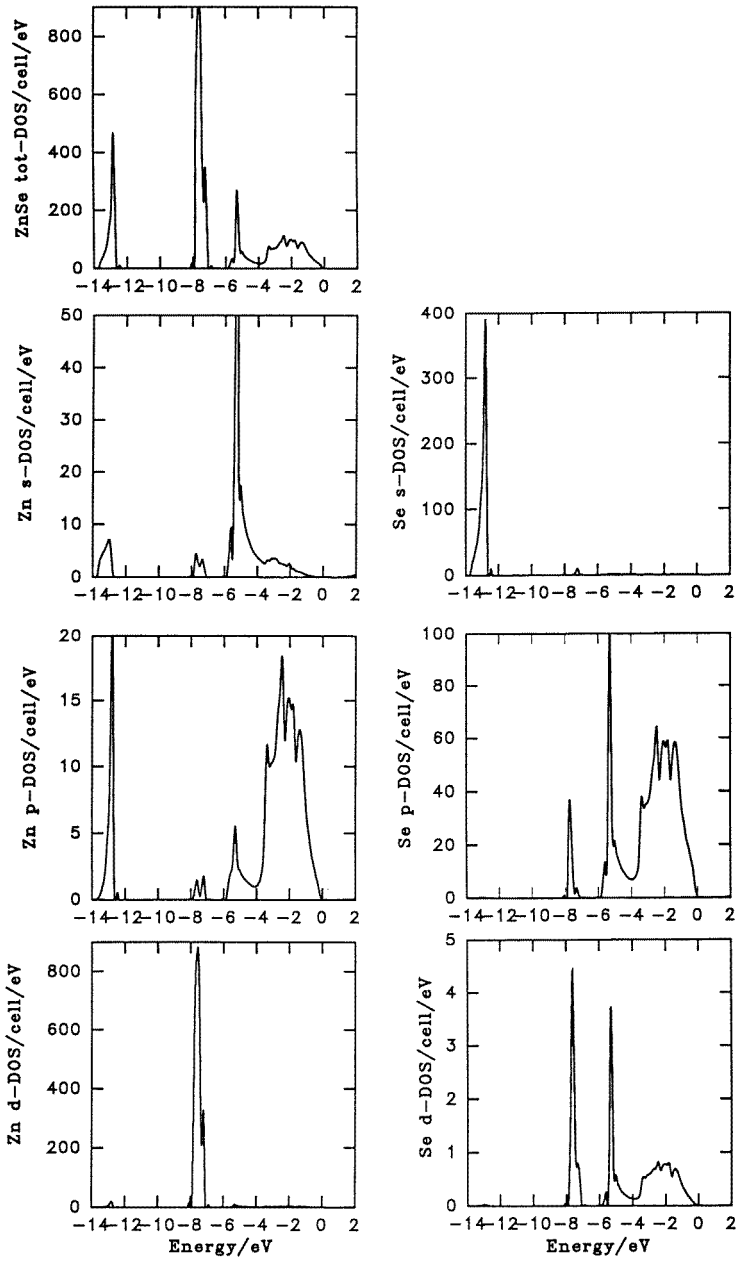

Figure 5. The tot-DOS of ZnSe and the partial s-, p- and d-DOS of Zn and Se in ZnSe.

the 4sp band. The width of this occupied part is 11.3 eV in pure Zn. In ZnS and ZnSe the band structure is split into three separate subbands. The total width of the occupied region in ZnS and ZnSe is 13.3 eV and 13.6 eV, respectively. The overall shapes of the total DOS of ZnS and ZnSe are quite similar. However, there are differences in the positions and intensities of the main peaks of the DOS. The lowest and central subbands of ZnSe are at

lower energies by 0.3 eV and 0.5 eV compared to those of ZnS, respectively.

Since the occupied part of the DOS is wider in ZnSe than in ZnS, the binding energies of the subbands are larger in ZnSe than in ZnS. The binding energy of the S (Se) 3s (4s) band is 12.1 eV (12.7 eV). The binding energy of the 3d band in pure Zn is 8.3 eV whereas in ZnS (ZnSe) it is 6.5 eV (7.1 eV). The two lowest subbands in ZnSe are narrower than in ZnS. This decrease in the width is 0.3 eV for the lowest occupied section and 0.1 eV for the central section. Contrary to the case for the two lowest subbands, the highest subband becomes slightly broader when going from ZnS to ZnSe. This broadening is 0.3 eV. Since this shift of the subbands to lower energies is accompanied with the narrowing of the two lowest subbands, the gaps between the different occupied sections of the DOS are increased when S is replaced by Se. This increase is 0.4 eV and 0.5 eV for the lower and higher band gap, respectively.

By considering the partial DOS curves in figures 3–5 we can analyse the total DOS curves in more detail. The lowest peak of the DOS in both compounds consists mainly of the S or Se s states with a small contribution coming from the Zn s and p states. In the central peak region the main contribution comes from the Zn d states with a few per cent contribution coming from the S or Se p states and a small contribution from all other states. The highest occupied part consists mainly of the S or Se p states, but there is a significant contribution from the Zn s and p states as well.

In pure Zn the hybridization between the d and s states and also between the d and p states is quite strong. In ZnS and ZnSe this kind of hybridization is weak. However, the hybridization of the Zn d states with the S or Se p states as well as with the S or Se d states is quite strong. Moreover, comparing figures 4 and 5 shows that the hybridization of the Zn d states with the Se states is considerably weaker than with the corresponding S states.

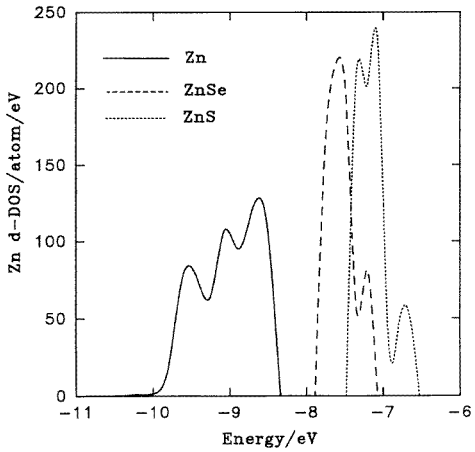

Figure 6. The d-DOS of Zn in Zn, ZnS and ZnSe.

In figure 6 the Zn d-DOS is shown for pure Zn and for Zn compounds. This figure reveals that both the position and the width of the Zn d band is changed significantly when going from one system to another. In pure Zn the width is almost double that found in ZnS and ZnSe. The overall shape of the Zn d-DOS in ZnS and ZnSe is almost the same, but the band shift from the pure Zn position is different for these two compounds. The shift obtained is 1.2 eV for ZnSe and 1.8 eV for ZnS.

5. Discussion

In the present work the electronic structure of Zn, ZnS and ZnSe is discussed on the basis of the x-ray emission measurements and the band-structure calculations. According to experiments and also to our calculations, ZnS and ZnSe are nonmetallic compounds. When we compare the partial DOSs of metallic Zn with those of Zn atoms in ZnS and ZnSe compounds we note some considerable differences. The most observable changes appear in the occupied s and p valence bands between metallic Zn and ZnS compound. For ZnS and ZnSe compounds the corresponding changes are quite small. In metallic Zn the total widths of the occupied s and p valence bands are 11.3 eV and within this energy region these bands are of continuous character. The situation is considerably different in ZnS and ZnSe compounds where the total widths of the occupied regions are 13.3 eV and 13.6 eV, respectively, and within these energy regions the band structure is split into three isolated subbands.

Table 1. The experimental and theoretical shifts of the Zn 3d-band binding energies. The reference energy is the 3d-band binding energy of pure Zn metal.

Compound	ΔE_{Expt}/eV	$\Delta E_{\mathrm{Theor}}$/eV
ZnS	1.3	1.8
ZnSe	0.9	1.2

The major differences in the DOS between Zn and ZnS and also between ZnS and ZnSe can be understood by considering the interactions between the atoms in these systems. When going from Zn to ZnS the Zn–Zn interaction decreases drastically. This reduction in the Zn–Zn interaction leads to the decreasing bandwidths. The width of the Zn d band is decreased about 40% and this decrease in the bandwidth is accompanied with the reduction of the binding energy of the Zn d band by 1.8 eV. The width of the Zn sp band is decreased by about 50%. The bottom of the Zn sp band is raised by 5.6 eV leading to the separation of the Zn d band from the Zn sp band. When going from ZnS to ZnSe the lattice parameter of the system is increased leading to the decreased Zn–Zn interaction. Hence the calculated width of the Zn d band for ZnSe is 10% smaller than that for ZnS. The narrowing of the bandwidth in this case is accompanied with the increasing of the binding energy of the Zn d band by 0.6 eV. The experimental and theoretical shifts of the Zn d-band binding energies are shown in table 1. In the case of Zn L$\alpha_{1,2}$ spectra one could expect narrowing of the d band on going from pure Zn metal to the compounds as well. However, the high-energy Coster–Kronig satellites could affect the shape of the experimental spectrum somewhat [17].

Figures 4 and 5 show that since the bottom of the Zn p band moves less downward than the top of the Zn d band, the gap between the Zn p and d bands increases when going from ZnS to ZnSe compound. In ZnS the width of this gap is 0.78 eV whereas in ZnSe it is 1.28 eV. According to our calculations the energy gaps between the valence and conduction bands of ZnS and ZnSe compounds are 2.0 eV and 1.3 eV, respectively. Experimental values for these gaps are 3.8 eV and 2.7 eV [18, 19]. The discrepancy between the experimental and theoretical results is mainly attributable to the local density approximation in the exchange–correlation potential [20].

For comparisons of the experimental XES spectra with the calculated results we consider more closely the Zn p- and d-DOS in ZnS and ZnSe compounds and in metallic Zn (see figures 3–5). In ZnS the hybridization between the Zn p and d states is much weaker than it is in pure Zn and it becomes slightly weaker on going from ZnS to ZnSe. This

suggests that the Zn 3d–4p hybridization is mainly due to the hybridization between the states belonging to the different Zn atoms. Above we have considered the changes only in Zn partial DOSs. However, considering the partial DOSs of S and Se atoms we notice in the compounds investigated the hybridization between S p and d states with Zn d states being much stronger than that for Se in ZnSe. This may be due to the lattice parameter in ZnSe being larger than that in ZnS. Moreover, since the binding energy of the s band in S (Se) is so large the hybridization between these s states and other states of this atom is negligible. The interaction between S (Se) s states and Zn states is quite strong in the calculations. In particular, there is a significant peak at -14 eV in the Zn p-DOS. However, this cannot be seen in the experimental spectrum which suggests a weak hybridization between the states belonging to the different atoms.

Comparing the calculated Se p-DOS (figure 5) with the experimental Se Kβ_2 spectrum in reference [21] suggests that although the Zn 3d–4p hybridization is clearly seen in the theoretical spectrum the effect seems to be rather small at the bottom of the experimental Se Kβ_2 spectrum. In pure Zn the 3d–4p hybridization appears to be quite strong in the theoretical p partial DOS at about the bottom of the band (figure 2). This effect is caused by the neighbouring atoms. However, the large broadening effects which are present in the experimental spectrum are not included in the calculated p-DOS. This broadening is caused by the finite lifetime of the Zn 1s core hole which has been created by an x-ray quantum in the initial state. The broadening effect is assumed to be of a Lorenzian type with the FWHM of 1.67 eV. In addition, the lifetime effect at the bottom of the band related to the valence electrons is quite large in the final state as well. Furthermore, the Auger broadening causing a tail at the bottom of the band is not included in the calculations either. One can assume that the transition matrix element is almost constant in this energy region [16] having only minor effects on the spectrum. The transition probability decreases rather weakly and almost linearly on going from the Fermi level to the higher binding energies leading to a slight suppression of the possible hybridization contribution to the peaks at the bottom of the band [22]. Owing to these properties the intensity of the possible hybridization effect on the Kβ_5 peak in the experimental spectrum is lower than expected on the basis of the calculations.

The contribution of the calculated 3d–4p hybridization at the bottom of the p-DOS decreases drastically when moving from pure Zn to ZnSe and ZnS compounds. This effect, however, cannot be seen as clearly in the experimental spectrum. Since the corresponding experimental features at the bottom of the K-emission band of the compounds do not decrease as much as is expected on the basis of the calculation of the partial p-DOS, the quadrupole transition would play a significant role in this connection. This suggests the interpretation of these features of the spectrum as being associated largely with the Kβ_5 transition.

6. Conclusions

The dipole selection rule makes it possible to analyse x-ray spectra by using calculated partial densities of states and gives the dominant contribution to the experimental K-emission band of pure Zn. However, comparing the experiments with the calculations one can suggest that the feature formed at the bottom of the experimental K-emission band of Zn and Zn compounds is associated to a considerable extent with the quadrupole transition. In addition, it is interesting to note, by comparing the calculated DOS of Zn and Zn compounds, that the hybridization between the 3d and 4p states in pure Zn would be mainly due to the states belonging to different atoms.

Acknowledgment

This work was financially supported by the Turku University Foundation.

References

[1] Haase M A, Qiu J, DePuydt J M and Cheng H 1991 *Appl. Phys. Lett.* **59** 1272–4
[2] Gaines J M, Drenten R R, Haberern K W, Marshall T, Mensz P and Petruzzello J 1993 *Appl. Phys. Lett.* **62** 2462–4
[3] Yu Z, Ren J, Lansari Y, Sneed B, Bowers K A, Boney C, Eason D B, Vaudo R P, Gossett K J, Cook J W Jr and Schetzina J F 1993 *Japan. J. Appl. Phys. Part 1* **32** 663–8
[4] Skriver H L 1984 *The LMTO Method (Springer Series in Solid State Sciences 41)* ed M Cardona and P Fulde (Berlin: Springer)
[5] Drahokoupil J and Šimůnek A 1974 *J. Phys. C: Solid State Phys.* **7** 610–8
[6] Lee G, Lee M H and Ihm J 1995 *Phys. Rev.* B **52** 1459–62
[7] Qteish A, Said R, Meskini N and Nazzal A 1995 *Phys. Rev.* B **52** 1830–8
[8] Markowski R, Piacentini M, Debowska D, Zimnal-Starnawska M, Lama F, Zema N and Kisiel A 1994 *J. Phys.: Condens. Matter* **6** 3207–19
[9] Agrawal B K, Yadav P S and Agrawal S 1994 *Phys. Rev.* B **50** 14 881–7
[10] Zakharov O, Rubio A, Blase X, Cohen M L and Louie S G 1994 *Phys. Rev.* B **50** 10 780–7
[11] Poon H C, Feng Z C, Feng Y P and Li M F 1995 *J. Phys.: Condens. Matter* **7** 2783–99
[12] Leiro J A 1987 *X-ray Spectrom.* **16** 177–9
[13] von Barth U and Hedin L 1972 *J. Phys C: Solid State Phys.* **5** 1629–42
[14] Sakurai J J 1976 *Advanced Quantum Mechanics* (New York: Addison-Wesley) p 41
[15] Krause M O and Oliver J H 1979 *J. Phys. Chem. Ref. Data* **8** 329
[16] Goodings D A and Harris R 1969 *J Phys. C: Solid State Phys.* **2** 1810–6
[17] Leiro J A 1988 *Phil. Mag. Lett.* **57** 189–93
[18] *Physics of II–VI and I–VII Compounds, Semimagnetic Semiconductors; Landolt–Börnstein New Series* 1982 Group III, vol 17, ed K-H Hellwege and O Madelung, Part b (New York: Springer)
[19] *Intrinsic Properties of Group IV Elements and III–V, II–VI and I–VII Compounds; Landolt–Börnstein New Series* 1982 Group III, vol 22, ed K-H Hellwege and O Madelung, Part a (New York: Springer)
[20] Das M P 1989 Density functional theory *Proc. 2nd Physics Summer School, Condensed Matter Physics (Canberra, 1989)* ed J Mahanty and M P Das (Singapore: World Scientific) p 111
[21] Drahokoupil J 1981 *Proc. Conf. in Physics (Jabłonna, 1981)* vol 5, ed J Auleytner and W Zahorowski (Warsaw: Polish Academy of Sciences, Institute of Physics) pp 60–73
[22] Lähdeniemi M, Ojala E, Suoninen E and Terakura I 1981 *J. Phys. F: Met. Phys.* **11** 1531–8